

Electron behavior in ion beam neutralization in electric propulsion: full particle-in-cell simulation

Hideyuki Usui, Akihiko Hashimoto and Yohei Miyake

Graduate School of System Informatics, Kobe University, 1-1 Rokkoudai, Nada, Kobe 657-8501, Japan

E-mail: h-usui@port.kobe-u.ac.jp

Abstract. By performing full Particle-In-Cell simulations, we examined the transient response of electrons released for the charge neutralization of a local ion beam emitted from an ion engine which is one of the electric propulsion systems. In the vicinity of the engine, the mixing process of electrons in the ion beam region is not so obvious because of large difference of dynamics between electrons and ions. A heavy ion beam emitted from a spacecraft propagates away from the engine and forms a positive potential region with respect to the background. Meanwhile electrons emitted for a neutralizer located near the ion engine are electrically attracted or accelerated to the core of the ion beam. Some electrons with the energy lower than the ion beam potential are trapped in the beam region and move along with the ion beam propagation with a multi-streaming structure in the beam potential region. Since the locations of the neutralizer and the ion beam exit are different, the above-mentioned bouncing motion of electrons is also observed in the direction of the beam diameter.

1. Introduction

As an interplanetary flight system, electric propulsion has been used for many spacecraft. Ion engine which is one of the typical electric propulsion systems gains the thrust by emitting heavy ions such as Xenon and Argon as an ion beam accelerated through grids in the electrostatic manner. To avoid the space-charge effect by excess emission of ions near the engine [1] and mitigate the spacecraft charging, thermal electrons are simultaneously released from a neutralizer attached in the vicinity of the ion engine location.

Ion beam emission and its neutralization by thermal electrons in electric propulsion is one of the most fundamental problems in spacecraft-plasma interactions. By emitting the same amount of electrons as the beam ions, the charge neutralization can be basically achieved in the spacecraft environment. However, because of large difference between electron and ion mass and dynamics, the charge neutralization between the two species does not simply occur outside the engine and the understanding of the neutralization process still remains at a rather primitive level. Although the previous works handled uniform ion beam which has an infinite cross section [2,3], we consider a situation in which an ion beam is emitted with a finite radius from a spacecraft [4-8] and simultaneously thermal electrons for the charge neutralization are released from a different position from the ion emitter [4]. Our focus is on the transient process of electron mixing to the ion beam in the very vicinity of the ion engine. To examine the transient process of the electron response in detail, we performed Particle-In-Cell [9,10] simulations in which both electrons and ions are treated as macro-particles and their dynamics are coupled with the electromagnetic field through electric current. In the



current study, we considered the electrostatic fields only in the simulations. In section 2, we introduce our simulation model and parameters used in the simulations. In section 3, we show some results obtained in the simulation in terms of electron behavior in the ion beam region. Section 4 contains the conclusion.

2. Simulation model

To examine the detail of electron behaviors in the ion beam region in the vicinity of a spacecraft, we performed three-dimensional full Particle-In-Cell (PIC) simulations by using our original software called “EMSES”[11], which we developed for the analysis of spacecraft-plasma interactions. Like other conventional PIC simulation codes, EMSES basically solves Maxwell’s equation to update the electromagnetic fields defined at spatial grid points by using the Finite-Difference Time-Domain (FDTD) method. In addition to the field components, dynamics of a large number of macro-particles representing electrons and ions which are distributed in the simulation space are updated by solving the equation of motion for each particle at each time step [9,10]. One of the unique features of EMSES is that it can define some internal conduction boundaries which represent to spacecraft conducting surfaces and solve the interactions with the surrounding plasma such as sheath formation near the surface and the spacecraft charging.

Figure 1 shows the three-dimensional simulation model used for the current study. An ion beam emitter and a neutralizer which releases thermal electrons are separately located on the spacecraft surface which is indicated in the figure as the injection plane. The location of the electron emitting neutralizer is set at the upper side of the ion emitter which is located in the middle of the injection plane. To shorten the calculation time in the simulation, we assumed protons as ions which are much lighter than the actual propellant such as Xenon. To keep the charge neutrality inside the spacecraft, total fluxes of the beam ions and thermal electrons are set to be the same to each other. We provide the beam velocity for the ions only and the electrons are thermally released from the neutralizer. We set the ratio of the electron thermal velocity v_{te} to the ion beam velocity v_{ibeam} as 1.25. The ion thermal velocity v_{ti} is much smaller than v_{ibeam} . Since the density of the background space plasma is small enough in comparison with that of the ion beam, we assumed no background plasma for simplicity. No interplanetary magnetic field is concerned in the current simulation. Since our aim is to examine

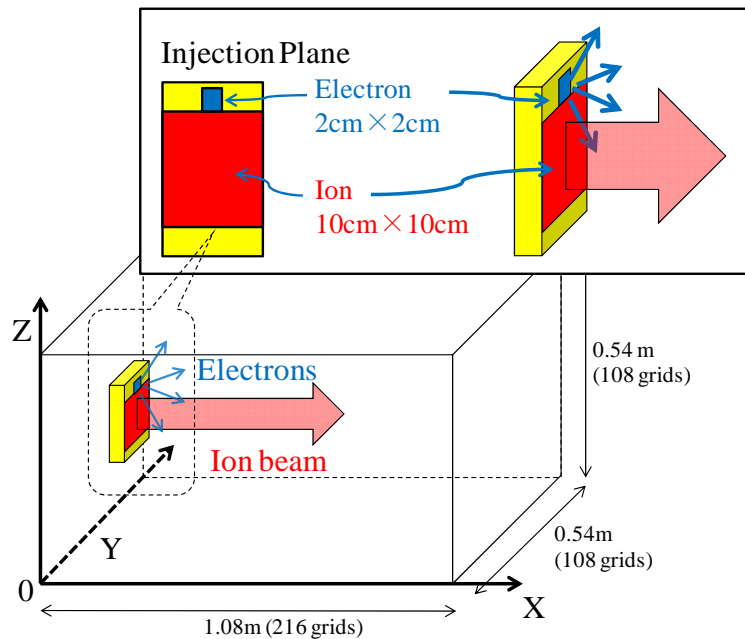


Figure 1. Simulation model.

electron response to the ion beam, we used EMSES in the electrostatic regime in which Poisson's equation is solved to update the electrostatic fields defined at the spatial grid points in the simulation space. The potential of the injection plane is treated as floating while the potential of the boundary surrounding the simulation space is fixed. To avoid the influence of the boundary potential to the plasma dynamics, we elongated the simulation space along the beam direction. We performed simulations up to the time when the beam reaches the simulation boundary.

3. Transient Response of Electrons

Figure 2 shows a bird's-eye view of spatial distribution of beam ions and thermal electrons measured at $\omega_{pe}t=400$ where ω_{pe} denotes the electron plasma frequency at the neutralizer. The ions and electrons emitted from the injection plane located near the left boundary of the simulation space are indicated in a large number of red and blue dots, respectively. Although the neutralizer which releases the thermal electrons is located at the upper side of the plane with respect to the ion beam emitter, the electrons are overall distributed in the ion beam region shown in red. If one carefully sees the electron distribution shown in blue, however, the distribution is not uniform particularly at the beam front as well as near the beam emitter.

In figure 3, we show temporal evolution of the ion beam and the thermal electrons in terms of density contour maps measured on an x - z plane including the center axis of the ion beam. Spatial scales and density values in the figure are normalized to the local Debye length λ_D and the maximum density n_{max} measured at the exit of the electron neutralizer, respectively. As clearly shown in the figure, the ion beam simply propagates away from the emitter as time elapsed. Although some diffusion of ions is seen at the beam front as in the bottom panel, the signature of the ion beam propagation is very straightforward because of ion's large inertia.

On the contrary, the emitted electrons show very complex signatures as shown in the right panels of figure 3. Thermal electrons are emitted from the upper side of the yellow body representing an ion engine. Note that the highest density is shown in blue in the right panels. It seems that the emitted

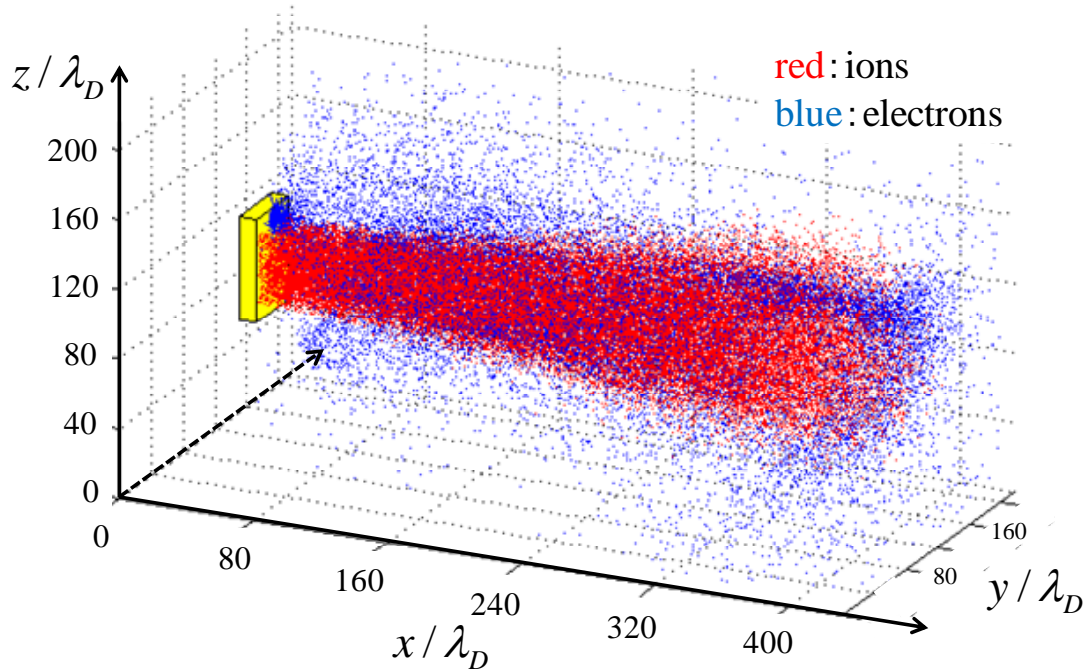


Figure 2. Spatial distribution of beam ions and thermal electrons emitted from a neutralizer measured at $\omega_{pe}t=400$.

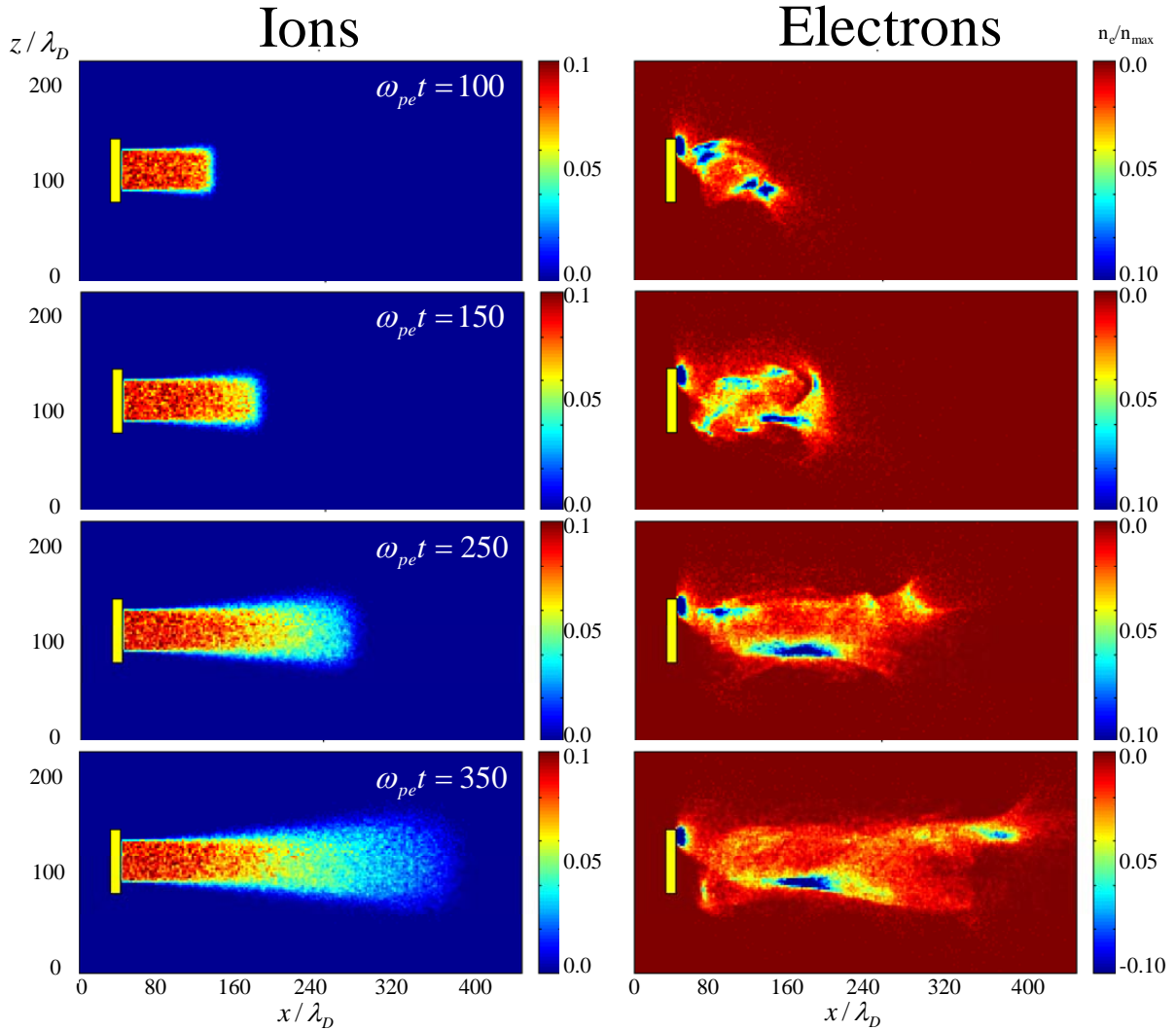


Figure 3. Contour maps for densities of ion beam and thermal electrons measured on an x - z plane including the center axis of the ion beam at different times.

electrons are overall attracted to the ion beam which has positive charges and they propagate along with the ion beam in the x direction to neutralize the positive ion charges. However, the electrons are not uniformly distributed in the beam region and the profile at each time seems asymmetric with respect to the ion beam direction. As shown in the third and fourth panels from the top, the electron density values become locally high at the surface surrounding the ion beam in the radial direction. The highest density region is constantly indicated at the location of the neutralizer attached at the upper side of the injection plane. In the beam region, however, the electron densities drastically change in time.

Figure 4 also shows density contour maps for the thermal electrons in different planes perpendicular to the ion beam propagation. Panels show the maps measured at $x/\lambda_D=80, 160, 240$, and 320 , respectively. As previously shown in the profiles along the beam direction, the electrons are overall distributed in the beam region also in the radial direction. The profiles are symmetric with respect to the center line of the y -axis. However, they are asymmetric between the upper and lower regions with respect to the center line of the z -axis. The maximum density is found at the lower side of the beam surface at $x/\lambda_D=160$ while it is around the top surface of the beam at $x/\lambda_D=320$ as shown in

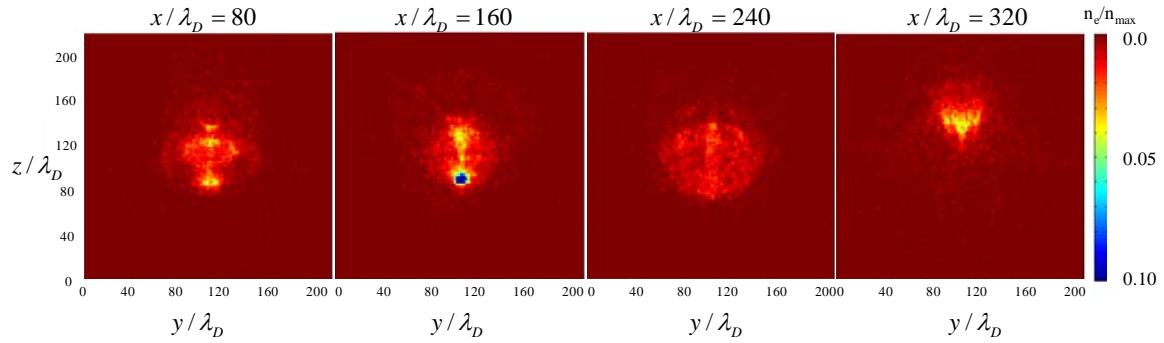


Figure 4. Contour maps for the electron densities measured on a y - z plane at the different locations along the x direction.

the most right panel. From these snapshots of the density profiles, it can be speculated that the thermal electrons released from the neutralizer make a kind of meandering or bouncing motion in the radial direction of the beam.

To understand the complex dynamics of the electrons shown in the previous figures, we examined the relation of the electrons to the electrostatic potential. In figure 5, we show a contour map of normalized electrostatic potential and the corresponding electron dynamics in an x - V_x phase space. The upper panel shows a snapshot of electrostatic potential measured on a x - z plane including the center axis of the ion beam measured at $\omega_{pet} = 300$. The potential values are color-coded and the high potential with respect to that of the vacuum region is shown in red. The potential values are plotted in terms of energy and they are normalized to the initial thermal energy of electrons. Because of large thermal velocity of the electrons the ion beam region is not perfectly neutralized and a positive potential region remains in the beam region as shown in the upper panel. Since the potential energy in the beam region is much larger than the initial electron thermal energy, most of the electrons released from the neutralizer are electrostatically trapped in the positive potential region.

In the lower panel of figure 5, we focus on the electron dynamics along the beam direction by showing an x - V_x phase diagram in which electrons are plotted in blue dots. The electrons emitted from the neutralizer are quickly accelerated along the beam direction and some fast electrons escape from the beam front, which is shown beyond $x/\lambda_D = 320$ in the panel. However, the most electrons are quickly decelerated at the beam front and are reflected back to the opposite direction to the beam propagation with negative velocities. They move toward the injection plane and are reflected back again toward the ion beam propagation with positive velocities. This bouncing motion of the electrons seems to be repeated multiple times in the beam region along the propagation direction. Although not displayed, as time elapses, the bouncing regions are elongated along the x direction in accordance with the ion beam propagation.

The bouncing period of the trapped electrons changes as the ion beam propagates away from the spacecraft. According to the conventional linear theory on the dynamics of electrons trapped in a potential well, the bouncing frequency ω_0 is approximately given as $\sqrt{e\Phi k^2/m}$ where e , m , Φ , and k denote the electron charge, mass, the electrostatic potential and its wavenumber, respectively. Since the potential region is elongated as the ion beam propagates, k becomes smaller and smaller as time elapses. Then ω_0 becomes correspondingly small and eventually the bouncing period becomes long. ϕ is another factor which determines ω_0 . ϕ is basically determined by the ion beam profile and may be slightly modified by the electron thermalization in the potential well. As shown in figure 5, the electron thermalization is caused by multiple bouncing motions in the potential well. These heated electrons may affect the potential structure as well as the ion beam propagation. However, as far as the

current simulation results are concerned, no influence on the ion beam propagation is observed. It may be because the simulation space and time is so limited and we could just focus on the initial stage of the ion beam emission.

Since the electron bouncing motions occur in the three-dimensional potential structure, which is unlike the conventional one-dimensional ideal situation, the bouncing motions are not so simple.

The potential region is also finite in the direction of the beam diameter and the potential has a peak at the core of the ion beam. Therefore, the electrons are also trapped in the radial direction of the beam. Non-uniform density profiles of electrons as shown in figure 3 and figure 4 are caused by the dynamic electron response to the ion beam potential. As soon as electrons are emitted from the neutralizer they are quickly attracted to the core of the ion beam and are initially accelerated to the negative z direction. Then most of them penetrate the core part of the ion beam with the maximum velocity. However, when the electrons pass through the beam core, they start to be decelerated and finally stagnate at the other side of beam surface in the radial direction. This stagnation can cause relatively high density found near the surface of the ion beam as shown in figure 3 and 4. The electrons again start to be accelerated back to the beam core by the electric field and this process seems to be repeated multiple times before the electrons reach the beam front.

Back to the electron motion along the beam propagation, we display a profile of velocity

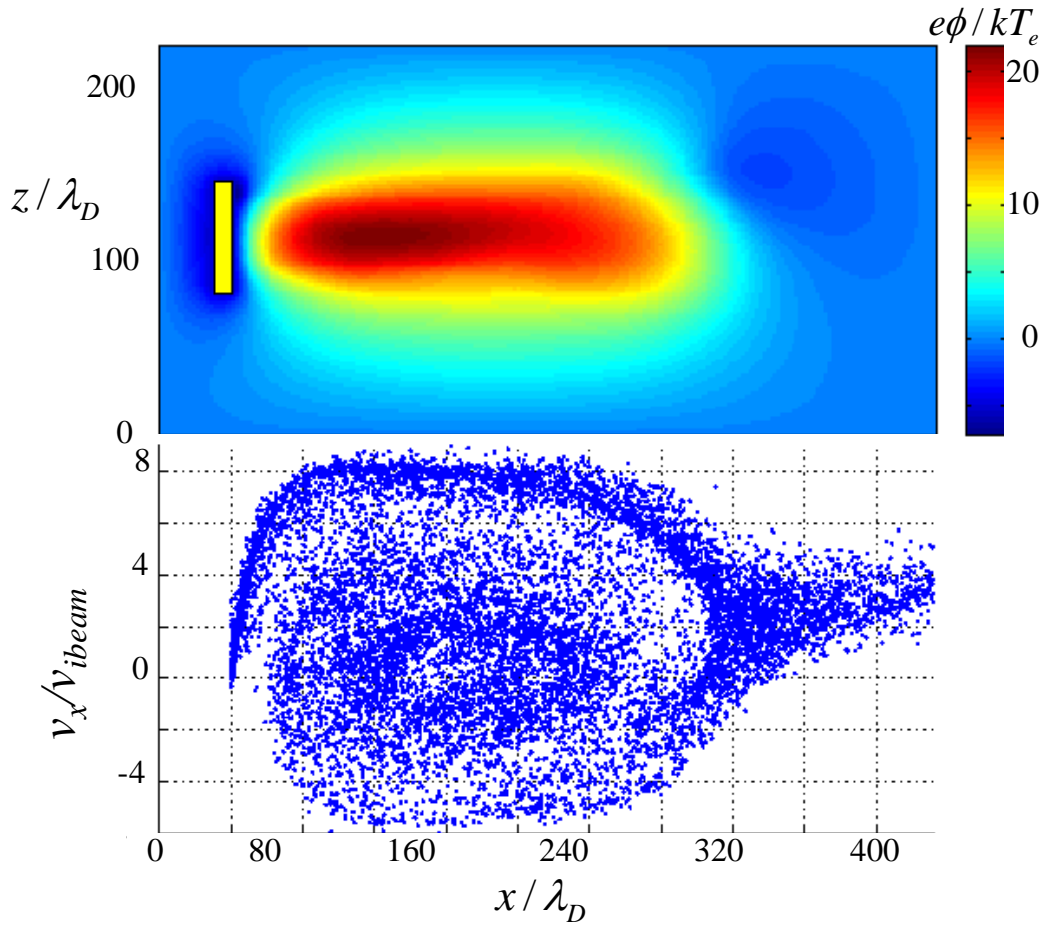


Figure 5. A contour map for electrostatic potential measured on a x - z plane including the ion beam propagation (upper panel) at $\omega_{pe}t = 300$ and the corresponding electron dynamics in a x - V_x phase space (lower panel).

distribution function of the electrons measured near the ion beam front in figure 6. As clearly shown, the function does not consist of a single Maxwellian but of two major components. One component has a peak which is located at positive velocity three times larger than v_{ibeam} . The other component which has a peak of negative velocity is owing to the electron reflection at the ion beam front. The velocity difference between the two peaks seems larger than the width of each distribution function. In such a situation, electron two-stream type instability may occur near the beam front and causes the local enhancement of the electric field which eventually heats electrons. Moreover, there may be some current-driven interactions between a cold ion beam and the accelerated electrons stated above. However, since the trapped electrons basically move back and forth along the beam direction in the potential well multiple times, the electron distribution overall tends to be smeared out and the clear velocity function which has two peaks can be seen only near the beam front as shown in figure 6. In other words, as shown in the lower panel of figure 5, the electron velocity distribution is not spatially uniform and rather varies much depending on the location along the beam direction. In such a situation, it may be difficult to observe electron two-stream instabilities because, according to the linear theory, the most unstable electrostatic mode has a wavelength which is much longer than the local region where the above velocity distribution is formed. This result basically agrees with the previous work [8] treating a local and finite beam emission. Meanwhile, the possibility of current-driven instabilities due to the difference between the cold ion beam and the accelerated electron component is not examined yet, which is left as a future work.

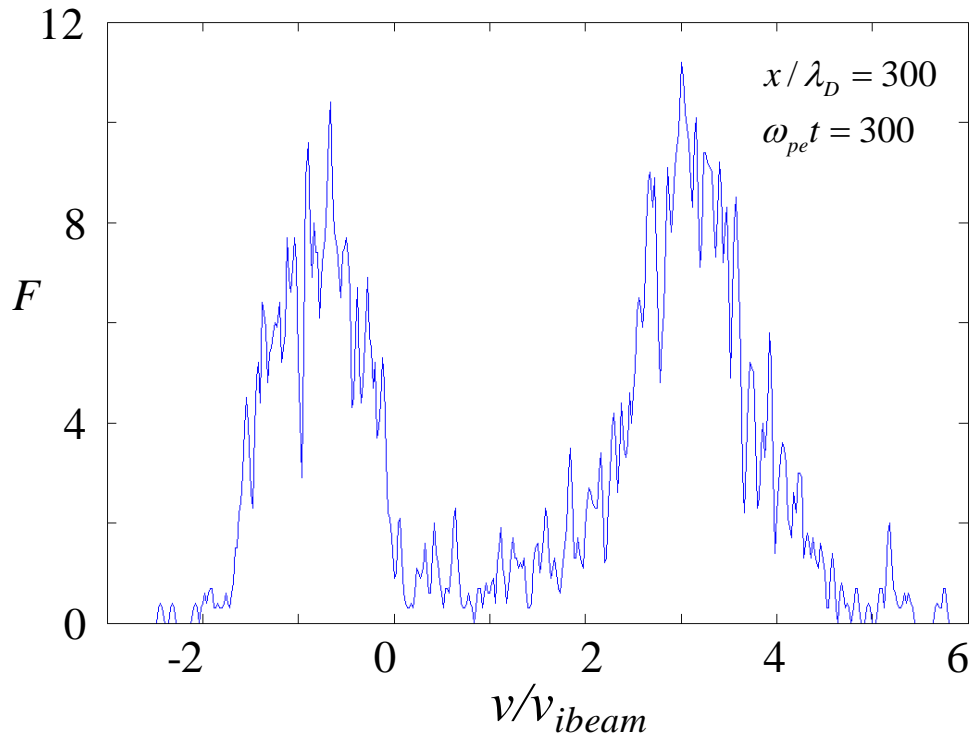


Figure 6. A distribution function of electron velocity along the ion beam propagation. F in the vertical axis is a normalized distribution function and the velocity v is normalized to v_{ibeam} .

4. Conclusion

We have examined the transient behavior of electrons released for ion beam neutralization in electric propulsion by performing full PIC simulations with EMSES. Unlike simple signature of ion beam propagation, we found that the behavior of thermal electrons emitted from the neutralizer is very complex. They basically propagate along with the ion beam to neutralize the positive charges of the ions. The electrons, however, are electrostatically trapped in a positive potential structure formed by the ion beam. The potential energy in the ion beam region is much larger than the initial thermal energy of electrons. The electrons released from the neutralizer are accelerated at the boundary of the potential well and move back and forth in the both directions parallel and perpendicular to the direction of the beam propagation. Although two major electron beam components are found particularly near the ion beam front, they are not uniform enough to cause electron two-stream instabilities. The electrostatic heating of electrons or the increase of the electron temperature is rather caused by the macroscopic trapping in the potential structure created in the whole region of the ion beam, not by the local beam instabilities. To examine the influence of electron trappings on the ion beam propagation, we need a much longer simulation space and time, which is left as a future work.

Acknowledgements

The computation in the present study was performed with the KDK system of Research Institute for Sustainable Human sphere (RISH) at Kyoto University.

References

- [1] Wang J and Lai S 1997 Virtual anode in ion beam emissions in space: Numerical simulations *J. Spacecraft Rockets* **34** pp 829-836
- [2] Buneman O and Kooyers G 1963 Computer Simulation of the Electron Mixing Mechanism in Ion Propulsion *J. AIAA(Am. Inst. Aeron. Astronaut.)* **1**(11) pp 2525-2528
- [3] Wadhwa R P, Buneman O, and Brauch D F 1965 Two-Dimensional Computer Experiments on Ion Beam Neutralization *J. AIAA(Am. Inst. Aeron. Astronaut.)* **3**(6) pp 1076-1081
- [4] Othmer C, Glassmeier K H, Schule J and Motschmann U 2000 Three dimensional simulations of ion thruster beam neutralization *Physics of Plasmas*, **7**(12) pp 5242-5251
- [5] Othmer C, Glassmeier K H, Motschmann U, Schule J and Frick Ch 2002 Numerical simulation of ion thruster-induced plasma dynamics. the model and initial results *Advances in Space Research* **29** pp 1357-1362.
- [6] Wheelock A, Gatsonis N and Cooke D 2003 Ion Beam Neutralization Processes for Electric Micropropulsion Applications *AIAA* 2003-5148
- [7] Brieda L and Wang J 2005 Modeling Ion Thruster Beam Neutralization Using a Fully Kinetic ES-PIC Code *AIAA* 2005-4045
- [8] Wang J, Chang O and Cao Y 2012 Electron-Ion Coupling in Mesothermal Plasma Beam Emission: Full Particle PIC Simulations *IEEE Transactions on Plasma Science* **40** pp 230 - 236
- [9] Birdsall C K and Langdon A B 1985 *Plasma Physics via Computer Simulation* McGraw-Hill Inc. New York
- [10] Omura Y and Matsumoto H 1993 *KEMPO1: Technical Guide to one-Dimensional Electro-magnetic Particle Code, Computer Space Plasma Physics: Simulation Techniques and Softwares* ed. By Matsumoto H and Omura Y Terra Scientific, Tokyo pp 21-65
- [11] Miyake Y and Usui H 2009 A new electromagnetic particle code for the analysis of conductive spacecraft-plasma interactions *Physics of Plasmas* **16** 062904